 SL, vol.8, no.2, pp.125-137, 2012

Radial Basis Functions Approximation Method for Numerical Solution of Good Boussinesq Equation

Marjan Uddin[1] **and Ghulam Kassem**[1]

Abstract: An interpolation method using radial basis functions is applied for the numerical solution of good Boussinesq equation. The numerical method is based on scattered data interpolation along with basis functions known as radial basis functions. The spatial derivatives are approximated by the derivatives of interpolation and a low order scheme is used to approximate the temporal derivative. The scheme is tested for single soliton and two soliton interaction. The results obtained from the method are compared with the exact solutions and the earlier works.

Keywords: Radial basis functions (RBFs), good Boussinesq equation, RBFs interpolation method.

1 Introduction

In the last decade, the theory of radial basis functions (RBFs) has enjoyed a great success as a scattered data interpolating technique. A radial basis function $\phi(x - x_j) = \phi(||x - x_j||)$ is a continuous spline which depends upon the separation distances of a subset of data centers $X \subset \Re^n$, $\{x_j \in X, j = 1,2,\ldots,N\}$. Due to the spherical symmetry about the centers x_j, the RBFs are called radial. The distances $||x - x_j||$ are usually taken to be the Euclidean metric. Hardy (1971) was the first to introduce a general scattered data interpolation method, called radial basis functions method for the approximation of two-dimensional geographical surfaces. In 1982 Franke (1982) in a review paper made a comparison among all the interpolation methods for scattered data sets available at that time, and the radial basis functions outperformed all the other methods regarding efficiency, stability and ease of implementations. Franke found that Hardy's multiquadrics (MQ) were ranked the best in accuracy, followed by thin plate splines (TPS). Despite MQ's excellent performance, it contains a shape parameter c, and the accuracy of MQ is greatly affected by the choice of shape parameter c whose optimal value is still unknown. Franke (1975) used the formula $c^2 = (1.25)^2 d^2$ where d is the mean distance from

[1] Department of Basic Sciences and Islamiat, KPK University of Engineering, Peshawar, Pakistan.

each data point to its nearest neighbor. Hickernell and Hon (1998); Golberg, Chen, and Karur (1996) had successfully used the technique of cross-validation to obtain an optimal value of the shape parameter. In 1990 radial basis functions scheme was introduced by Kansa (1990a) to solve partial differential equations. The existence, uniqueness and convergence of this method was discussed by Micchelli (1986); Madych and Nelson (1990); Franke and Schaback (1997). It was studied by Micchelli in 1986 that for distinct interpolation points system obtained in multiqudric (MQ) method is always solvable. In the past decade RBFs interpolation method have received increased attention for numerically solving partial differential equations (PDEs) on irregular domains by global collocation approach (see, Kansa (1990b); Hickernell and Hon (1998); Fasshuer (1999); Larsson and Forenberg (2003) ect.). When proper attention is paid to boundaries, these methods can be spectrally accurate, they generally result in having to solve a large, ill-conditioned, dense linear system. Some attempts have been made to resolve this problem (see Fasshuer (1999); Kansa and Hon (2000); Ling and Kansa (2005) and references therein). The RBFs scheme is truly a meshfree method which does not require the generation of a mesh, and since the MQ is infinitely differentiable, we can approximate the higher order spatial derivative directly by computing the derivative of the basis functions. Due to the generality and simplicity, such technique and its variation have been successfully applied to many areas [Fasshuer (1999); Fasshauer, Khaliq, and Voss (2004); Hon, Cheung, Mao, and Kansa (1999); Hon and Mao (1999); Li, Hon, and Chen (2002); Power and Barraco (2002); Franke and Schaback (1997); Zhou, Hon, and Li (2003); Li, Chen, and Pepper (2003); Haq and Uddin (2010)]. However the stability issues have limited the use of RBFs for time dependent problems and adapting the methods for non-linear equations has proven to be difficult.

In this work, we use RBFs approximation method for the numerical solution of good Boussinesq equation. The good Boussinesq equation is a nonlinear equation which describes shallow water waves, propagating in both directions, is given by

$$\frac{\partial^2 u(x,t)}{\partial t^2} = \frac{\partial^2 u(x,t)}{\partial x^2} + q\frac{\partial^4 u(x,t)}{\partial x^4} + \frac{\partial^2 (u^2(x,t))}{\partial x^2}, \quad (x,t) \in [a,b] \times [0,T]. \tag{1}$$

with the initial conditions

$$u(x,0) = u_1(x), u_t(x,0) = u_2(x), \tag{2}$$

and the boundary conditions

$$u(a,t) = g_1(t), u(b,t) = g_2(t). \tag{3}$$

Where $|q| = 1$ is a real parameter, the value $q = -1$ leads to good Boussinesq or well-posed equation (see [Bratsos (2008)] and the references there in), whereas for $q = 1$ gives bad boussinesq equation or ill-posed equation [Boussinesq (1871, 1872)]. The good Boussinesq equation describes motion of long waves in the shallow water under gravity. The Boussinesq equation has been solved numerically by finite difference method [Bratsos (1998); Bratsos, Tsitouras, and Natsis (2005); Bratsos (2008); Ismail and Bratsos (2003); El-Zoheiry (2003); Saucez, Wouwer, Schiesser, and Zegeling (2004)], pseudospectral method [Daripa and Hua (1999)], finite element method [Pani and Saranga (1997)], method of lines [Bratsos (1998); Saucez, Wouwer, Schiesser, and Zegeling (2004)].

The structure of the present paper is organized as follows. In Section 2, the meshfree method for good Boussinesq equation and the stability of the scheme have been discussed. Section 3, is devoted to the numerical tests of the method on the problems related to the good Boussinesq equation. In Section 4, the results have been concluded.

2 Analysis of the method

In this section, we consider a general time dependent boundary value problem

$$\frac{\partial u}{\partial t} + \mathscr{L}u = f(x,t), x \in \Omega, \quad \mathscr{B}u = g(x,t), \quad x \in \partial\Omega \tag{4}$$

where $\mathscr{L}$ is the spatial derivative and $\mathscr{B}$ boundary operators. Ω and $\partial\Omega$ represent interior and boundary of the domain respectively. We use the scheme for spatial derivatives in the following form

$$\frac{U^{n+1} - U^n}{\Delta t} + \mathscr{L}U^n = f(x, t^{n+1}) \tag{5}$$

In the above equation Δt is the time step size, U^n (n is non-negative integer) is the approximate solution at time $t^n = n\Delta t$. Let $\{x_i\}_{i=1}^{N_d}$ and $\{x_i\}_{i=N_d+1}^{N}$ be respectively interior and boundary points among the collocation points $\{x\}_{i=1}^{N}$ in the domain. The solution of equation (4) can be approximated by

$$U^n(x_i) = \sum_{j=1}^{N} \psi(r_{ij})\lambda_j^n, i = 1, 2, \ldots, N. \tag{6}$$

In the above equation $\psi(r_{ij})$ are radial basis functions with Euclidean norm $r_{ij} = ||x_i - x_j||$ between the points x_i and x_j and $\{\lambda_j\}_{j=1}^{N}$ are constants to be determined. From Equations (5) and (6), we can write

$$\sum_{j=1}^{N} \left(\frac{\psi(r_{ij})\lambda_j^{n+1} - \psi(r_{ij})\lambda_j^n}{\Delta t} + [\psi(r_{ij})]\lambda_j^n \right) = f(x, t^{n+1}), i = 1, 2, \ldots, N_d, \tag{7}$$

$$\sum_{j=1}^{N} \mathscr{B}(\psi(r_{ij}))\lambda_j^{n+1} = g(x_i, t^{n+1}), i = N_d + 1, \ldots, N. \tag{8}$$

The equations (7)-(8) are N equations in N unknowns $\{\lambda_j\}_{j=1}^{N}$ which can be solved by Gauss elimination method.

2.1 The good Boussinesq equation

We transform the good Boussinesq equation into coupled equations and is given by

$$\frac{\partial u(x,t)}{\partial t} = v(x,t), \frac{\partial v(x,t)}{\partial t} = \frac{\partial^2 u(x,t)}{\partial x^2} + q\frac{\partial^4 u(x,t)}{\partial x^4} + \frac{\partial^2 (u^2(x,t))}{\partial x^2}, (x,t) \in [a,b] \times [0,T] \tag{9}$$

with the boundary conditions

$$u(a,t) = f_1(t), u(b,t) = f_2(t), v(a,t) = g_1(t), v(b,t) = g_2(t), \quad t > 0, \tag{10}$$

and initial conditions

$$u(x,0) = f(x), v(x,0) = g(x), \quad a \le x \le b. \tag{11}$$

From equation (9) we can write

$$\left[\frac{U^{n+1} - U^n}{\Delta t}\right] = V^n, \quad \left[\frac{V^{n+1} - V^n}{\Delta t}\right] = [U_{xx}^n + qU_{xxxx}^n + 2U^n U_{xx}^n + 2(U_x^n)^2], \tag{12}$$

rearranging equation (12) we get

$$U^{n+1} = U^n + \Delta t V^n, V^{n+1} = V^n + \Delta t(U_{xx}^n + qU_{xxxx}^n + 2U^n U_{xx}^n + 2(U_x^n)^2) \tag{13}$$

where $t^{n+1} = t^n + \Delta t$. The RBFs approximations for the solutions u and v of equations in (9) are given by

$$U^n(x_i) = \sum_{j=1}^{N} \lambda_{1j}^n \psi(r_{ij}), \quad V^n(x_i) = \sum_{j=1}^{N} \lambda_{2j}^n \psi(r_{ij}), i = 1, 2, \ldots, N \tag{14}$$

By using equation (13) along with the boundary conditions given in equation (10), the system of equations in equation (13) can be written in matrix form as

$$\mathbf{A}\lambda_1^{n+1} = \mathbf{A}\lambda_1^n + \Delta t \mathbf{V}^n + \mathbf{f}^{n+1}, \mathbf{A}\lambda_2^n + \Delta t(\mathbf{U_{xx}^n} + q\mathbf{U_{xxxx}^n} + 2\mathbf{U^n}\mathbf{U_{xx}^n} + 2(\mathbf{U_x^n})^2) + \mathbf{g}^{n+1}, \tag{15}$$

where $\mathbf{A} = [\psi(r_{ij})]_{i,j=1}^{N}$. In more compact form we can write equations in (15) as

$$\lambda_1^{n+1} = \mathbf{A}^{-1}\mathbf{A}\lambda_1^n + \mathbf{A}^{-1}\mathbf{F}^{n+1}, \lambda_2^{n+1} = \mathbf{A}^{-1}\mathbf{A}\lambda_2^n + \mathbf{A}^{-1}\mathbf{G}^{n+1}. \tag{16}$$

Where

$$\begin{aligned}
\lambda_i^{\mathbf{n}+1} &= [\lambda_{i1}^{n+1}, \lambda_{i2}^{n+1}, \lambda_{i3}^{n+1}, \ldots, \lambda_{iN}^{n+1}]^T, i = 1,2,\\
\mathbf{f}^{\mathbf{n}+1} &= [f_1^{n+1}, 0, 0, \ldots, f_2^{n+1}]^T,\\
\mathbf{g}^{\mathbf{n}+1} &= [g_1^{n+1}, 0, 0, \ldots, g_2^{n+1}]^T,\\
\mathbf{F}^{\mathbf{n}+1} &= [\mathbf{f}^{\mathbf{n}+1} + \Delta t \mathbf{V}^{\mathbf{n}}],\\
\mathbf{G}^{\mathbf{n}+1} &= [\mathbf{g}^{\mathbf{n}+1} + \Delta t(\mathbf{U}^{\mathbf{n}}_{\mathbf{xx}} + q\mathbf{U}^{\mathbf{n}}_{\mathbf{xxxx}} + 2\mathbf{U}^{\mathbf{n}}\mathbf{U}^{\mathbf{n}}_{\mathbf{xx}} + 2(\mathbf{U}^{\mathbf{n}}_{\mathbf{x}})^2)].
\end{aligned}$$

Equations in (14) can be written in matrix form as

$$\mathbf{U}^n = \mathbf{A}\lambda_1^n, \mathbf{V}^n = \mathbf{A}\lambda_2^n, \text{ or } \mathbf{U}^{n+1} = \mathbf{A}\lambda_1^{n+1}, \mathbf{V}^{n+1} = \mathbf{A}\lambda_2^{n+1} \tag{17}$$

Using the values λ_i^n and λ_i^{n+1}, $(i = 1,2)$ from equation (16) in equation (17), we get

$$\mathbf{U}^{n+1} = \mathbf{A}\mathbf{A}^{-1}\mathbf{A}\mathbf{A}^{-1}\mathbf{U}^n + \mathbf{A}\mathbf{A}^{-1}\mathbf{F}^{\mathbf{n}+1}, \mathbf{V}^{n+1} = \mathbf{A}\mathbf{A}^{-1}\mathbf{A}\mathbf{A}^{-1}\mathbf{V}^n + \mathbf{A}\mathbf{A}^{-1}\mathbf{G}^{\mathbf{n}+1}. \tag{18}$$

From here we can find the solution at any time level n.

It is shown by Hon and Schaback (n.d) that for the Euler time-stepping the system of equation will be stable if it satisfy the condition $\delta t \le C(\delta x)^2$, where C is a constant. Hence in our case the scheme in equation (18) will be stable if we keep time step size δt small enough to satisfy the above condition. This fact can be seen from Table 5, where the accuracy increases with a decrease in time step size δt.

3 Numerical examples

In this section, we apply the proposed method for the numerical solution of GB equation. The accuracy of the meshfree method is tested in terms of L_2, L_∞ error norms and the conservation of energy $M(t)$ [Bratsos (2008)] of GB equation. These error norms and energy are defined as

$$\begin{aligned}
L_2 &= ||U-u||_2 = \left[\delta x \sum_{j=1}^{N} (U-u)^2\right]^{1/2},\\
L_\infty &= ||U-u||_\infty = \max_j |U-u|.
\end{aligned}$$

$$M(t) = \int_{-\infty}^{\infty} u(x,t)\,dx, \tag{19}$$

where U and u denote the numerical and exact solution respectively. The test problems are given below.

3.1 Problem 1. Single soliton:

We consider GB equation (1) as system of two equations given in (9). The exact [Bratsos (2008)] solutions of the equations in (9) are given as

$$u(x,t) = -\alpha \operatorname{sech}^2\left(\sqrt{\frac{\alpha}{6}}(x-x_0-Ct)\right) - \left(\beta+\frac{1}{2}\right) \tag{20}$$

$$v(x,t) = -2\alpha C \operatorname{sech}^2\left(\sqrt{\frac{\alpha}{6}}(x-x_0-Ct)\right)\tanh\left(\sqrt{\frac{\alpha}{6}}(x-x_0-Ct)\right),$$

$$C = \pm[-2(\beta+\alpha/3)]^{1/2}.$$

Table 1: Error norms and energy constant for single soliton, when $\Delta t = 0.0002$, $N = 241$, $C = 0.868332$, $\alpha = 0.369$, $\beta = -0.5$ in $[-40, 80]$ corresponding to problem 1.

	t	1.2	3.6	9	36	72
MQ ($c=2$)	L_∞	1.904E-005	1.699E-005	2.801E-005	9.529E-005	2.130E-004
	L_2	1.881E-006	7.480E-006	1.840E-005	1.205E-004	4.738E-004
	$M(t)$	-2.975905	-2.975909	-2.975916	-2.975981	-2.975788
	Amp.	0.368970	0.368656	0.368252	0.367786	0.369170
GA($c=1$)	L_∞	1.904E-005	1.700E-005	2.805E-005	9.540E-005	2.085E-004
	L_2	1.397E-009	3.222E-009	4.725E-009	6.924E-005	3.484E-004
	M(t)	-2.975903	-2.975903	-2.975903	-2.975952	-2.975699
	Amp.	0.368970	0.368656	0.368252	0.367786	0.369166
Ref. [Bratsos (1998)]	L_∞		0.920E-001	0.943E-001		
Ref. [Bratsos, Tsitouras, and Natsis (2005)]	L_∞	0.269E-002			0.141E+000	0.130E+000
	L_2	0.370E-002			0.251E+000	0.323E+000
Ref. [Bratsos (2008)]	L_∞				0.103E-003	0.146E-003

The initial conditions $u(x,0)$ and $v(x,0)$, the boundary conditions $u(a,t)$, $u(b,t)$, $v(a,t)$ and $v(b,t)$ are obtained from the exact solutions in equation (20). We solved the problem over the spatial domain $-40 \le x \le 80$. In our computations we used three types of radial basis functions, the multiquadric ($\psi(r) = \sqrt{c^2+r^2}$, c is a shape parameter), the Gaussian ($\psi(r) = \exp(-cr^2)$, c is a shape parameter) and the spline basis ($\psi(r) = r^5$). In order to demonstrate the accuracy of the method, we calculated the L_∞ the L_2 error norms, the energy $M(t)$ and the amplitude of the approximate solution at different times and are given in Tables 1-2. The results are compared with the relevant works in references [Bratsos (1998); Bratsos, Tsitouras, and Natsis (2005); Bratsos (2008)] in Tables 1-2. In comparison the present method performed better than the methods given in references [Bratsos (1998); Bratsos, Tsitouras, and Natsis (2005); Bratsos (2008)]. The L_∞, L_2 error norms are also calculated for different values of the parameters α, C and are given in Tables 3.

In Table 4 the effect of time step size δt is shown. It is observed that the solution accuracy improves with a decrease in time step size δt. It is shown in Table 5 and figure 2 that the optimal values of MQ and GA shape parameters are in the intervals $(0, 4.16)$, and $(0, 32)$ respectively. The motion of solitary wave is shown at times different times in Fig. 1.

Table 2: Error norms for single soliton for different values of α and C, when $\Delta t = 0.00002$, $N = 241$, MQ($c = 2$), $\beta = -0.5$ in $[-40, 80]$ corresponding to problem 1.

α	C	t	$L_\infty(MQ)$	$Ł_\infty(GA)$	L_∞([Bratsos (2008)])
1.2	0.44721	67.7	1.576E-003	3.138E-001	blow-up
1.	5 0	20.7	3.130E-001	5.621E-006	blow-up

Table 3: Error norms for single soliton for different values of α and C, when $\Delta t = 0.0002$, $N = 241$, MQ($c = 2$), GA($c = 1$), $\beta = -0.5$ at $t = 1$ in $[-40, 80]$ corresponding to problem 1.

α	C	$L_\infty(MQ)$	$L_\infty(GA)$	$L_\infty(r^7)$
0.15	0.94868	1.909E-006	1.909E-006	2.615E-006
0.5	0.81650	1.471E-005	1.471E-005	2.985E-004
1.2	0.44721	2.232E-005	2.244E-005	5.351E-003
1.5	0	1.134E-006	1.382E-008	1.121E-002

Table 4: Error norms and energy constant versus time step size Δt for single soliton, when MQ($c = 2$), GA($c = 1$), $\beta = -0.5$, $N = 241$, $\alpha = 0.369$, $C = 0.868332$ at time $t = 1$ in $[-40, 80]$ corresponding to problem 1.

Δt	$L_\infty(MQ)$	$L_\infty(GA)$	$\lvert M(t) - M(0)\rvert$
0.1	4.426E-003	4.426E-003	2.3083E-007
0.01	4.589E-004	4.589E-004	2.2094E-007
0.001	4.604E-005	4.604E-005	2.2093E-007
0.0001	4.612E-006	4.615E-006	2.2093E-007
0.00001	8.757E-007	8.763E-007	2.2093E-007

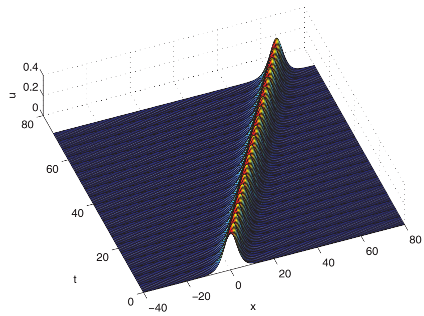

(a) Surface plot of approximate u

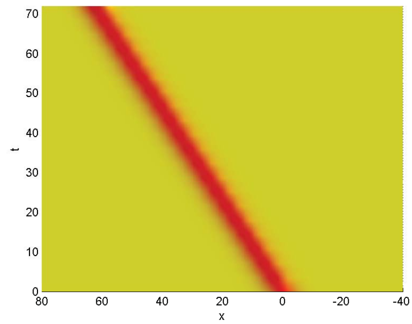

(b) Contour plot of approximate u

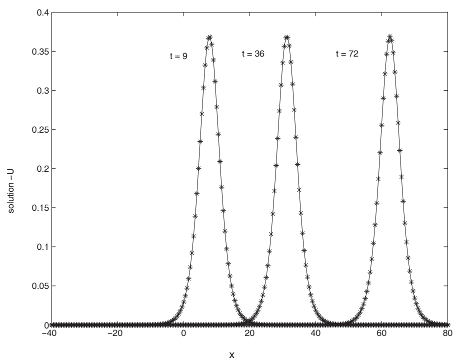

(c) Exact u (dotted curve), approximate u (full line)

Figure 1: Single soliton: when $\Delta = 0.0002$, $N = 241$, $c = 2$, $C = 0.868332$, $\alpha = 0.369$, $\beta = -0.5$ in $[-40, 80]$, up to time $t = 72$, corresponding to problem 1.

3.2 *Problem 2. Two soliton interaction:*

We consider the following initial conditions

$$u(x,0) = -\sum_{i=1}^{2}\left[\alpha_i \mathrm{sech}^2\left(\sqrt{\frac{\alpha_i}{6}}(x-x_i) - \left(\beta_i + \frac{1}{2}\right)\right)\right], \tag{21}$$

$$v(x,0) = -2\sum_{i=1}^{2}\alpha_i C_i \mathrm{sech}^2\left(\sqrt{\frac{\alpha_i}{6}}(x-x_i)\right)\tanh\left(\sqrt{\frac{\alpha_i}{6}}(x-x_i)\right)$$

$$C_i = \pm[-2(\beta_i + \alpha_i/3]^{1/2}, i = 1,2.$$

The boundary conditions are chosen as $u(a,0) = 0$, $u(b,0) = 0$, $v(a,0) = 0$ and $v(b,0) = 0$. The above initial conditions are the sum of two solitary waves initially centered at $x_1 = -10$ and $x_2 = 40$ with the amplitudes α_1 and α_2. The two waves moves toward each other, with the speeds C_1 and C_2 respectively. In Figs. 3-4, the interaction of two waves with equal and unequal amplitudes are shown. The interaction of the two waves is elastic, and after interaction the waves retain their shape and amplitudes are shown in Fig. 3-4. We also calculated the energy constant for

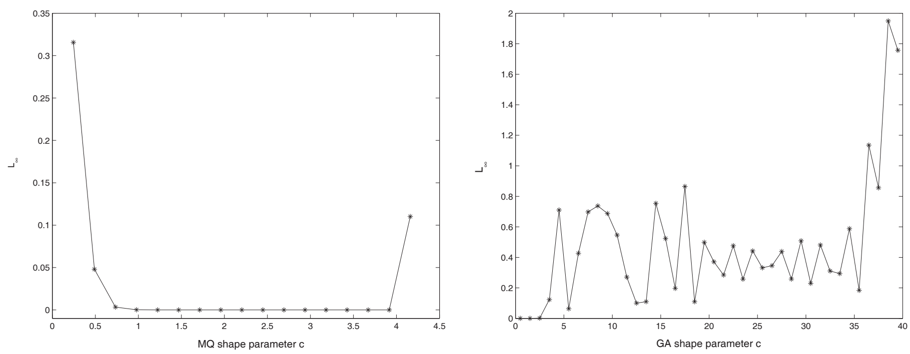

(a) L_∞ error norm against MQ(c) (b) L_∞ error norm against MQ(c)

Figure 2: Single soliton: when time step size Δt, $t = 1$, $N = 241$, $C = 0.868332$, $\alpha = 0.369$, $\beta = -0.5$ in $[-40, 80]$, corresponding to problem 1.

two solitons interaction which remains constant in time interval $[0, 60]$ see Table 6.

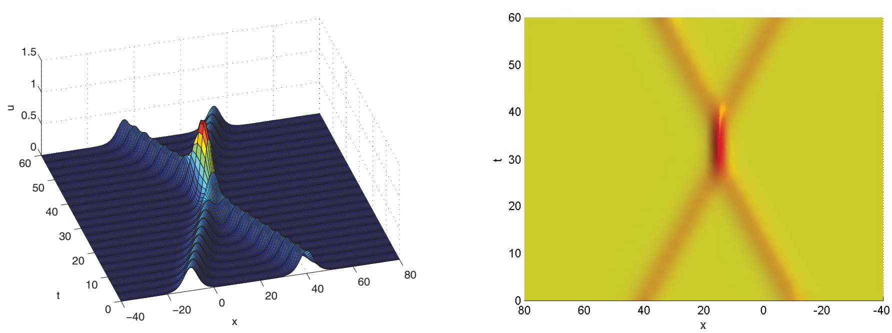

(a) Interaction of two waves with equal amplitudes (b) Contour plot of interaction of two waves

Figure 3: Two solitons interaction: when $\Delta t = 0.0004$, $N = 241$, MQ($c = 2$), $C_1 = 0.868332$, $C_2 = -0.868332$, $x_1 = -10$, $x_2 = 40$, $\alpha_1 = 0.369$, $\alpha_2 = 0.369$, $\beta_1 = -0.5$, $\beta_2 = -0.5$ in $[-40, 80]$, up to time $t = 60$, corresponding to problem 2.

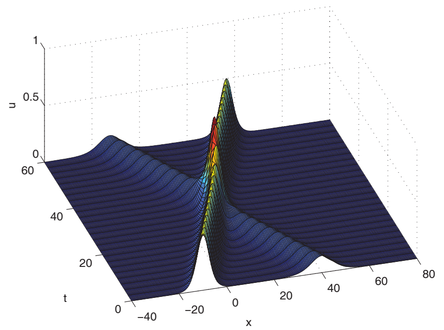

(a) Interaction of two waves with unequal amplitudes

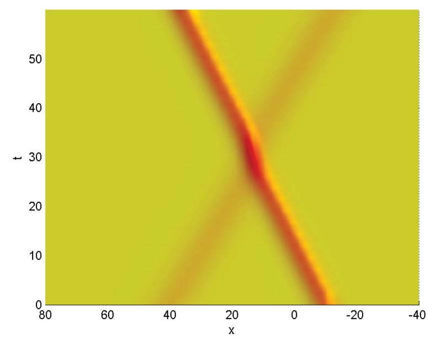

(b) Contour plot of interaction of two waves

Figure 4: Two solitons interaction: when $\Delta t = 0.0004$, $N = 241$, MQ($c = 2$), $C_1 = 0.81650$, $C_2 = -0.94868$, $x_1 = -10$, $x_2 = 40$, $\alpha_1 = 0.5$, $\alpha = 0.15$, $\beta_1 = -0.5$, $\beta_2 = -0.5$, in $[-40, 80]$ up to time $t = 60$, corresponding to problem 2.

Table 5: Error norms and energy constant versus MQ shape parameter c for single soliton, when $\Delta t = 0.0002$, $N = 241$, $\beta = -0.5$, $\alpha = 0.369$, $C = 0.868332$ at time $t = 1$ in $[-40, 80]$ corresponding to problem 1.

MQ		GA	
c	L_∞	c	L_∞
0.244720	3.156E-001	0.50	9.219E-006
0.489440	4.801E-002	1.50	9.130E-006
0.734160	3.302E-003	2.50	1.683E-003
0.978880	2.014E-004	3.50	1.232E-001
1.223600	4.373E-006	4.50	7.103E-001
1.468320	8.313E-006	20.50	3.709E-001
1.713040	9.156E-006	25.50	3.318E-001
1.957760	9.215E-006	12.50	1.001E-001
2.202480	9.219E-006	16.50	1.965E-001
2.447200	9.219E-006	20.50	3.709E-001
2.691920	9.219E-006	24.50	4.424E-001
2.936640	9.219E-006	28.50	2.575E-001
3.181360	9.219E-006	32.50	3.108E-001
4.160240	1.102E-001	36.50	1.135E+000

4 Conclusion

In this paper, the RBFs approximation is applied for the numerical solution of good Boussinesq equation. We split the problem as system of two equations. We only

Table 6: Energy constant for two solitons interaction, when $\Delta t = 0.0004$, $N = 241$, MQ($c = 2$), GA($c = 1$), $C_1 = 0.868332$, $C_2 = -0.868332$, $x_1 = -10$, $x_2 = 40$, $\alpha_1 = 0.369$, $\alpha_2 = 0.369$, $\beta_1 = -0.5$, $\beta_2 = -0.5$ in $[-40, 80]$, corresponding to problem 2.

	MQ	GA
t	$M(t)$	$M(t)$
0	-5.9518	-5.9518
15	-5.9519	-5.9518
35	-5.9521	-5.9520
50	-5.9523	-5.9544

displayed the solution u. The technique used in this paper provides an efficient alternative for the solution of higher PDEs in time as well as in space. From application viewpoints the implementation of this method is very simple and straightforward.

References

Boussinesq, M. J. (1871): Thorie de lintumescence appele onde solitaire ou de translation se propageant dans un canal rectangulaire. *C. R. Acad. Sc. Paris*, vol. 72, pp. 755–759.

Boussinesq, M. J. (1872): Thorie des ondes et des remous qui se propagent le long dun canal rectangulaire horizontal, en communiquant au liquide contenu dans ce canal des vitesses sensiblemant perielles de la surface au fond. *J. Math. Pures Appl. Ser.*, vol. 17, no. 2, pp. 55–108.

Bratsos, A. G. (1998): The solution of the boussinesq equation using the method of lines. *Comput. Methods Appl. Mech. Engrg.*, vol. 157, pp. 33–44.

Bratsos, A. G. (2008): Solitary-wave propagation and interactions for good boussinesq equation. *Int.J. Comput. Math.*, vol. 85, no. 9, pp. 1431–1440.

Bratsos, A. G.; Tsitouras, C.; Natsis, D. G. (2005): Linearized numerical schemes for the boussinesq equation. *Appl. Num. Anal. Comp. Math.*, vol. 2, no. 1, pp. 34–53.

Daripa, P.; Hua, W. (1999): A numerical study of an ill-posed boussinesq equation arising in water waves and nonlinear lattices: filtering and regularization techniques. *Appl. Math. Comput.*, vol. 101, no. 2, pp. 159–207.

El-Zoheiry, H. (2003): Numerical investigation for the solitary waves interaction of the good boussinesq equation. *Appl. Numer. Math.*, vol. 45, pp. 161–173.

Fasshauer, G. E.; Khaliq, A. Q. M.; Voss, D. A. (2004): Using meshfree approximation for multi-asset american option problems. *J. Chines Institute Engineers*, vol. 27, pp. 563–571.

Fasshuer, G. E. (1999): Solving partial differential equations with radial basis functions: multilevel methods and smoothing. *Adv. Comput. Math.*, vol. 11, pp. 139–159.

Franke, C.; Schaback, R. (1997): Convergence orders of meshless collocation methods using radial basis functions. *Adv. Comput. Math.*, vol. 8, no. 4, pp. 381–399.

Franke, R. (1975): critical comparison of some methods for interpolation of scattered data. Technical Report NPS-53-79-003, Naval Postgraduate School, 1975.

Franke, R. (1982): Scattered data interpolation: Tests of some methods. *Math. Comp.*, vol. 38, pp. 181–200.

Golberg, M. A.; Chen, C. S.; Karur, S. (1996): Improved multiquadric apporoxmation for partial differential equations. *Eng. Anal. Bound. Elem.*, vol. 18, pp. 9–17.

Haq, S.; Uddin, M. (2010): Rbfs approximation method for kawahara equation. *Eng. Anal. Bound. Elem.*

Hardy, R. L. (1971): Multiquadric equations of topography and other irregular surfaces. *J. Geo-Phys. Res.*, vol. 176, pp. 1905–1915.

Hickernell, F. J.; Hon, Y. C. (1998): Radial basis function approximation of the surface wind field from scattered data. *International Journal of applied science and Computations*, vol. 4, no. 3, pp. 221–247.

Hon, Y. C.; Cheung, K. F.; Mao, X. Z.; Kansa, E. J. (1999): Multiquadric solution for shallow water equations. *ASCE J. Hydraulic Eng.*, vol. 125, pp. 524–533.

Hon, Y. C.; Mao, X. Z. (1999): A radial basis function method for solving options pricing model. *Financial Eng.*, vol. 8, pp. 31–49.

Hon, Y. C.; Schaback, R. (n.d): Meshless kernel techniques for the heat equations. *Schabak web page*. Preprint.

Ismail, M. S.; Bratsos, A. G. (2003): A predictor-corrector scheme for the numerical solution of the boussinesq equation. *J. Appl. Math. Comput.*, vol. 13, no. 12, pp. 1127.

Kansa, E. J. (1990): Multiquadrics scattered data approximation scheme with applications to computational fluid-dynamics. i. surface approximations and partial derivative estimates. *Appl. Math. Comput.*, vol. 19, pp. 127–145.

Kansa, E. J. (1990): A scattered data approximation scheme with applications to computational fluid-dynamics- ii: solutions to parabolic and elliptic partial differential equations. *Comput. Math. Appl.*, vol. 19, pp. 147–161.

Kansa, E. J.; Hon, Y. C. (2000): Circumventing the ill-conditioning problem with multiquadric radial basis functions: applications to elliptic partial differential equations. *Comput. Math. Appl.*, vol. 39, pp. 123–137.

Larsson, E.; Forenberg, B. (2003): A numerical study of some radial basis functions based solution methods for elliptic pdes. *Comput. Math. Appl.*, vol. 46, pp. 891–902.

Li, J.; Chen, Y.; Pepper, D. (2003): Radial basis function method for 1-d and 2-d groundwater contaminant transport modeling. *Comput. Mech.*, vol. 32, pp. 10–15.

Li, L.; Hon, Y. C.; Chen, C. S. (2002): Numerical comparisons of two meshless methods using radial basis functions. *Eng. anal. Bound. Elem*, vol. 26, pp. 205–225.

Ling, L.; Kansa, E. J. (2005): A least-squeres preconditioner for radial basis functions collocation methods. *Adv. Comput. Math.*, vol. 23, pp. 31–54.

Madych, W. R.; Nelson, S. A. (1990): Multivariate interpolation and conditionally positive definite functions ii. *Math. Comput.*, vol. 54, pp. 211–30.

Micchelli, C. A. (1986): Interpolation of scatterted data: distance matrix and conditionally positive definite functions. *Construct. Approx.*, vol. 2, pp. 11–22.

Pani, A.; Saranga, H. (1997): Finite element galerkin method for the good boussinesq equation. *Nonlinear Anal.*, vol. 29, no. 8, pp. 937956.

Power, H.; Barraco, V. (2002): A comparison analysis between unsymmetric and symmetric radial basis function collocation methods for the numerical solution of partial differential equations. *Comput. Math. appl.*, vol. 43, pp. 551–583.

Saucez, P.; Wouwer, A. V.; Schiesser, W. E.; Zegeling, P. (2004): Method of lines study of nonlinear dispersive waves. *J. Comput. Appl. Math.*, vol. 168, pp. 413423.

Zhou, X.; Hon, Y. C.; Li, J. (2003): Overlapping domain decomposition method by radial basis functions. *Appl. Numer. Math.*, vol. 44, pp. 243–257.